Research Article | Vol. 25, No. 5 | 6 Mar 2017 | OPTICS EXPRESS 4665

Optics EXPRESS

Optical vector analysis based on asymmetrical optical double-sideband modulation using a dual-drive dual-parallel Mach-Zehnder modulator

TING QING,[1] SHUPENG LI,[1] MIN XUE,[1,*] WEI LI,[2] NINGHUA ZHU,[2] AND SHILONG PAN[1,*]

[1]*Key Laboratory of Radar Imaging and Microwave Photonics, Ministry of Education, Nanjing University of Aeronautics and Astronautics, Nanjing, 210016, China*
[2]*State Key Laboratory on Integrated Optoelectronics, Institute of Semiconductors, Chinese Academy of Sciences, Beijing 100083, China*
[*]*xuemin@nuaa.edu.cn, pans@ieee.org*

Abstract: A novel approach to perform optical vector analysis (OVA) is proposed and experimentally demonstrated with carrier-shifted optical double-sideband (ODSB) modulation based on a dual-drive dual-parallel Mach-Zehnder modulator (DD-DPMZM). The proposed method has a doubled measurement range as compared with the conventional OVA based on optical single sideband modulation (OSSB), and a much simpler and more robust configuration as compared with the previously-reported ODSB-based OVA. In addition, the proposed scheme does not generate any undesirable spikes in the measurement results. The transmission response of a sampled fiber Bragg grating in a range of 80 GHz is measured with a resolution of less than 667 kHz by using 40-GHz microwave components. The influence of the unideal frequency-shifted optical carrier generation in the DD-DPMZM on the measurement error is also investigated.

© 2017 Optical Society of America

OCIS codes: (120.0120) Instrumentation, measurement, and metrology; (300.6320) Spectroscopy, high-resolution; (060.5625) Radio frequency photonics.

References and links

1. T. Niemi, M. Uusimaa, and H. Ludvigsen, "Limitations of phaseshift method in measuring dense group delay ripple of fiber Bragg gratings," IEEE Photonics Technol. Lett. **13**(12), 1334–1336 (2001).
2. G. D. VanWiggeren, A. R. Motamedi, and D. M. Barley, "Single-scan interferometric component analyzer," IEEE Photonics Technol. Lett. **15**(2), 263–265 (2003).
3. P. Yves, A. Maryse, B. Guillaume, and P. Marie-Josée, "Ultra-narrowband notch filtering with highly resonant fiber bragg gratings," in *Bragg Gratings, Photosensitivity, and Poling in Glass Waveguides*, (Optical Society of America, 2010), paper BTuC3.
4. I. S. Grudinin, V. S. Ilchenko, and L. Maleki, "Ultrahigh optical Q factors of crystalline resonators in the linear regime," Phys. Rev. A **74**(6), 063806 (2006).
5. E. Voges, O. Ostwald, B. Schiek, and A. Neyer, "Optical phase and amplitude measurement by single sideband homodyne detection," IEEE J. Quantum Electron. **18**(1), 124–129 (1982).
6. J. E. Román, M. Y. Frankel, and R. D. Esman, "Spectral characterization of fiber gratings with high resolution," Opt. Lett. **23**(12), 939–941 (1998).
7. T. Kawanishi, T. Sakamoto, and M. Izutsu, "Optical filter characterization by using optical frequency sweep technique with a single sideband modulator," IEICE Electron. Express **3**(3), 34–38 (2006).
8. M. Sagues and A. Loayssa, "Swept optical single sideband modulation for spectral measurement applications using stimulated Brillouin scattering," Opt. Express **18**(16), 17555–17568 (2010).
9. Z. Tang, S. Pan, and J. Yao, "A high resolution optical vector network analyzer based on a wideband and wavelength-tunable optical single-sideband modulator," Opt. Express **20**(6), 6555–6560 (2012).
10. M. Xue, Y. Zhao, X. Gu, and S. Pan, "Performance analysis of optical vector analyzer based on optical single-sideband modulation," J. Opt. Soc. Am. B **30**(4), 928 (2013).
11. M. Xue, S. Pan, C. He, R. Guo, and Y. Zhao, "Wideband optical vector network analyzer based on optical single-sideband modulation and optical frequency comb," Opt. Lett. **38**(22), 4900–4902 (2013).
12. C. Zhu, J. Chang, P. Wang, W. Wei, S. Zhang, Z. Liu, and G. Peng, "Acquisition of phase-shift fiber grating spectra with 23.5 femtometer spectral resolution using DFB-LD," Opt. Express **21**(25), 31540–31547 (2013).

#283481 https://doi.org/10.1364/OE.25.004665
Journal © 2017 Received 22 Dec 2016; revised 14 Feb 2017; accepted 15 Feb 2017; published 21 Feb 2017

Optics EXPRESS

13. M. Wang and J. P. Yao, "Optical vector network analyzer based on unbalanced double-sideband modulation with improved measurement accuracy," IEEE Photonics Technol. Lett. **25**(8), 753–756 (2013).
14. M. Xue, S. Pan, and Y. Zhao, "Accuracy improvement of optical vector network analyzer based on single-sideband modulation," Opt. Lett. **39**(12), 3595–3598 (2014).
15. W. Li, W. T. Wang, L. X. Wang, and N. H. Zhu, "Optical vector network analyzer based on single-sideband modulation and segmental measurement," IEEE Photonics J. **6**(2), 7901108 (2014).
16. M. Xue, S. Pan, and Y. Zhao, "Accurate optical vector network analyzer based on optical single-sideband modulation and balanced photodetection," Opt. Lett. **40**(4), 569–572 (2015).
17. T. Qing, M. Xue, M. Huang, and S. Pan, "Measurement of optical magnitude response based on double-sideband modulation," Opt. Lett. **39**(21), 6174–6176 (2014).
18. T. Qing, S. Li, M. Xue, and S. Pan, "Optical vector analysis based on double-sideband modulation and stimulated Brillouin scattering," Opt. Lett. **41**(15), 3671–3674 (2016).
19. G. H. Smith, D. Novak, and Z. Ahmed, "Overcoming chromatic-dispersion effects in fiber-wireless systems incorporating external modulators," IEEE Trans. Microw. Theory Tech. **45**(8), 1410–1415 (1997).

1. Introduction

Optical vector analysis (OVA) is a technology to measure frequency responses, including magnitude, phase and polarization responses, of optical devices, which is essential for device fabrication and system design. The optical vector analyzers are conventionally implemented based on modulation phase-shift approach [1] or interferometry method [2], which characterize the frequency responses by sweeping the wavelength of a wavelength-swept laser source. Restricted by the low wavelength accuracy and stability of wavelength-swept laser sources, they have a relatively poor resolution (typically several hundreds of MHz), which is too low to extract the frequency responses of high-fineness optical devices, such as fiber Bragg gratings (FBGs) with a 3-dB bandwidth of 9 MHz [3] and high-Q optical resonators [4]. To achieve ultrahigh-resolution measurement, the OVA based on optical single-sideband (OSSB) modulation is proposed and demonstrated [5–16], which potentially has a sub-Hz resolution. However, the key challenge of the OSSB-based OVA is to implement a high-performance OSSB modulator with a wide sweeping range, high linearity and large sideband suppression ratio (SSR) [9]. Since such OSSB modulators are hard to be achieved, the performance, especially the measurement range, accuracy and dynamic range, of the OSSB-based OVA is restricted [10].

Recently, an OVA based on optical double-sideband (ODSB) modulation is proposed [17, 18], which characterizes the optical devices using both of the two first-order sidebands without frequency aliasing by shifting the frequency of the optical carrier. Compared with the OSSB-based OVA, the ODSB-based OVA has a doubled measurement range, and better nonlinearity immunity which leads to a higher accuracy and a larger dynamic range. However, to achieve the carrier-shifted ODSB signal, in [17] the optical carrier and the two sidebands had to be separated so that a frequency shift can be introduced to the optical carrier without affecting the two sidebands. In this case, however, the phase response cannot be accurately measured due to the large phase noise between the two separated optical paths. In [18], the carrier-shifted ODSB signal was generated with the assistance of stimulated Brillouin scattering (SBS) effects in an optical fiber. Since only one transmission path is required, both the magnitude and phase responses can be measured. The key problems associated with this approach are the complicated configuration, polarization sensitivity of the SBS effect, and obvious spectral spikes in the measurement results due to the gain or absorption spectra of the SBS.

To overcome the above problems, we report in this paper a novel ODSB-based OVA incorporating a dual-drive dual-parallel Mach-Zehnder modulator (DD-DPMZM). In the DD-DPMZM, one sub-MZM produces a wavelength-sweeping ODSB signal, and the other sub-MZM generates a wavelength-fixed OSSB signal by employing a 90° hybrid coupler [19]. The remained first-order sideband in the wavelength-fixed OSSB signal is served as the frequency-shifted carrier, which is combined with the wavelength-sweeping ODSB signal at the output port of the DD-DPMZM. When propagating through an optical device under test (ODUT), the two wavelength-sweeping first-order sidebands carry out the frequency responses

Optics EXPRESS

at both sides of the optical carrier. In a photodetector (PD), two RF signals with different frequencies are generated by beating the two first-order sidebands and the frequency-shifted carrier. By extracting the magnitudes and phases of the two RF signals, the frequency responses of the ODUT are obtained. Since the frequency-shifted carrier and the sweeping sidebands are produced in a single electro-optic modulator (EOM), they are phase related and the phase response can be accurately measured. It should be noted that high-order sidebands would not introduce measurement errors, since the beat notes of the high-order sidebands have a different frequency from those beat by the frequency-shifted carrier and the two desired sidebands. But the residual sideband in the wavelength-fixed OSSB signal would influence on the measurement accuracy and the dynamic range, which is investigated and discussed in this paper.

2. Principle

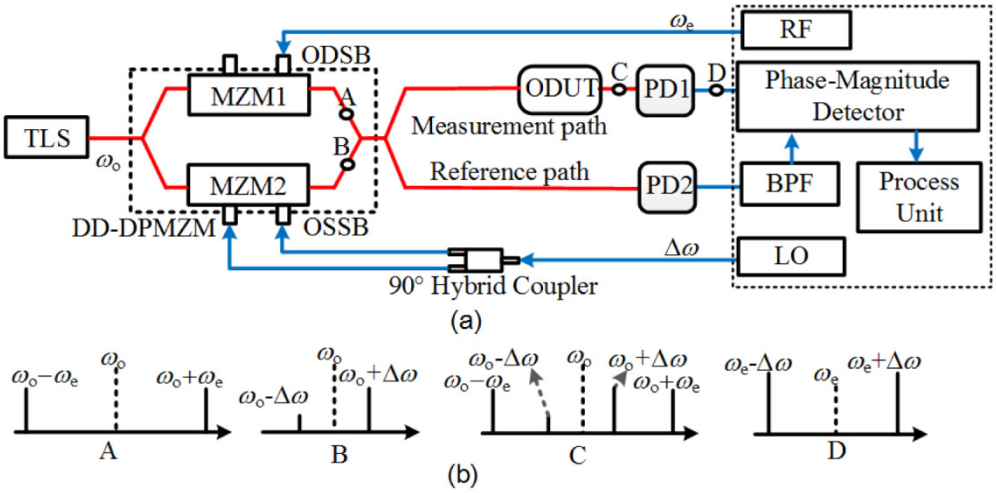

Fig. 1. (a) The schematic diagram of the proposed ODSB-based OVA; (b) spectra of the signals at different points. TLS, tunable laser source; MZM, Mach-Zehnder modulator; DD-DPMZM, dual-drive dual-parallel MZM; ODUT, optical device under test; PD, photodetector; BPF, band-pass filter; RF, radio frequency; LO, local oscillator.

Figure 1(a) shows the schematic diagram of the proposed ODSB-based OVA. A lightwave with an angular frequency of ω_o from a tunable laser source (TLS) is sent to a DD-DPMZM, in which it is divided into two portions. One portion is modulated by a frequency-swept RF signal with a frequency of ω_e in MZM1, generating an ODSB signal having two sweeping sidebands with frequencies of $\omega_o - \omega_e$ and $\omega_o + \omega_e$, respectively. The other portion is modulated by a frequency-fixed local oscillator (LO) signal with a frequency of $\Delta\omega$ in MZM2 to produce an OSSB signal, where the desired first-order sideband has a frequency of $\omega_o + \Delta\omega$ and the suppressed sideband has a frequency of $\omega_o - \Delta\omega$. At the output port of the DD-DPMZM, the two portions are combined to form a carrier-shifted ODSB signal, which can be expressed as

$$E(\omega) = a_{-1}\delta\left[\omega-(\omega_o-\omega_e)\right]+a_{+1}\delta\left[\omega-(\omega_o+\omega_e)\right] + b_{-1}\delta\left[\omega-(\omega_o-\Delta\omega)\right]+b_{+1}\delta\left[\omega-(\omega_o+\Delta\omega)\right] \quad (1)$$

where a_{+1} and a_{-1} are the complex amplitudes of the sweeping ± 1st-order sidebands of the wavelength-sweeping ODSB signal, and b_{+1} and b_{-1} are the complex amplitudes of the desired + 1st-order sideband and the suppressed −1st-order sideband of the wavelength-fixed OSSB signal, which are the desired frequency-shifted carrier and the unwanted frequency-shifted carrier, respectively. Residual optical carriers and higher-order sidebands are ignored because

Optics EXPRESS

the beat notes produced by the frequency-shifted carrier and them have different frequencies from those of the signals of interest, which can be easily removed in the signal processing stage.

When the signal in (1) goes through an ODUT, the magnitudes and phases of the sweeping ± 1st-order sidebands and the frequency-shifted carriers are changed according to the transmission function of the ODUT. The electric field of the optical signal can be written as

$$\begin{aligned} E_{\mathrm{m}}(\omega) &= E(\omega)\cdot H(\omega) \\ &= a_{-1}H(\omega_{\mathrm{o}}-\omega_{\mathrm{e}})\delta\left[\omega-(\omega_{\mathrm{o}}-\omega_{\mathrm{e}})\right]+a_{+1}H(\omega_{\mathrm{o}}+\omega_{\mathrm{e}})\delta\left[\omega-(\omega_{\mathrm{o}}+\omega_{\mathrm{e}})\right] \\ &+b_{-1}H(\omega_{\mathrm{o}}-\Delta\omega)\delta\left[\omega-(\omega_{\mathrm{o}}-\Delta\omega)\right]+b_{+1}H(\omega_{\mathrm{o}}+\Delta\omega)\delta\left[\omega-(\omega_{\mathrm{o}}+\Delta\omega)\right] \end{aligned} \quad (2)$$

where $H(\omega)=H_{\mathrm{sys}}(\omega)\cdot H_{\mathrm{ODUT}}(\omega)$, $H_{\mathrm{sys}}(\omega)$ and $H_{\mathrm{ODUT}}(\omega)$ are the transmission functions of the measurement system and the ODUT, respectively.

After square-law detection in a PD (PD1), a photocurrent carrying the frequency responses of $H(\omega)$ is achieved, given by

$$\begin{aligned} &i_{\mathrm{m}}(\omega_{\mathrm{e}}-\Delta\omega)=\eta a_{+1}b_{+1}^{*}H(\omega_{\mathrm{o}}+\omega_{\mathrm{e}})H^{*}(\omega_{\mathrm{o}}+\Delta\omega)+\eta a_{-1}^{*}b_{-1}H^{*}(\omega_{\mathrm{o}}-\omega_{\mathrm{e}})H(\omega_{\mathrm{o}}-\Delta\omega),\ \text{if } \omega_{\mathrm{e}}>\Delta\omega \\ &i_{\mathrm{m}}(\Delta\omega-\omega_{\mathrm{e}})=\eta a_{+1}^{*}b_{+1}H^{*}(\omega_{\mathrm{o}}+\omega_{\mathrm{e}})H(\omega_{\mathrm{o}}+\Delta\omega)+\eta a_{-1}b_{-1}^{*}H(\omega_{\mathrm{o}}-\omega_{\mathrm{e}})H^{*}(\omega_{\mathrm{o}}-\Delta\omega),\ \text{if } \omega_{\mathrm{e}}<\Delta\omega \\ &i_{\mathrm{m}}(\omega_{\mathrm{e}}+\Delta\omega)=\eta a_{-1}^{*}b_{+1}H^{*}(\omega_{\mathrm{o}}-\omega_{\mathrm{e}})H(\omega_{\mathrm{o}}+\Delta\omega)+\eta a_{+1}b_{-1}^{*}H(\omega_{\mathrm{o}}+\omega_{\mathrm{e}})H^{*}(\omega_{\mathrm{o}}-\Delta\omega) \end{aligned} \quad (3)$$

where η is the responsivity of PD1. On the right hand of (3), the first term is the photocurrent carrying the frequency responses, and the second term is the measurement error introduced by the unwanted frequency-shifted carrier.

To remove the responses of the measurement system, a calibration step has to be performed, in which the ODUT is removed and the two test ports are directly connected (i.e. $H_{\mathrm{ODUT}}(\omega)=1$). Since $|b_{+1}|>>|b_{-1}|$ for the wavelength-fixed OSSB signal produced by MZM2, the unwanted frequency-shifted carrier induced measurement error can be ignored. Thus, the photocurrent in the calibration step is

$$\begin{aligned} &i_{\mathrm{cal}}(\omega_{\mathrm{e}}-\Delta\omega)=\eta a_{+1}b_{+1}^{*}H_{\mathrm{sys}}(\omega_{\mathrm{o}}+\omega_{\mathrm{e}})H_{\mathrm{sys}}^{*}(\omega_{\mathrm{o}}+\Delta\omega),\ \text{if } \omega_{\mathrm{e}}>\Delta\omega \\ &i_{\mathrm{cal}}(\Delta\omega-\omega_{\mathrm{e}})=\eta a_{+1}^{*}b_{+1}H_{\mathrm{sys}}(\omega_{\mathrm{o}}+\omega_{\mathrm{e}})H_{\mathrm{sys}}^{*}(\omega_{\mathrm{o}}+\Delta\omega),\ \text{if } \omega_{\mathrm{e}}<\Delta\omega \\ &i_{\mathrm{cal}}(\omega_{\mathrm{e}}+\Delta\omega)=\eta a_{-1}^{*}b_{+1}H_{\mathrm{sys}}(\omega_{\mathrm{o}}-\omega_{\mathrm{e}})H_{\mathrm{sys}}^{*}(\omega_{\mathrm{o}}+\Delta\omega) \end{aligned} \quad (4)$$

According to (3) and (4), the transmission function of the ODUT can be obtained, which can be expressed as

$$\begin{aligned} &H_{\mathrm{ODUT}}^{\mathrm{m}}(\omega_{\mathrm{o}}+\omega_{\mathrm{e}})=\frac{i_{\mathrm{m}}(\omega_{\mathrm{e}}-\Delta\omega)}{i_{\mathrm{cal}}(\omega_{\mathrm{e}}-\Delta\omega)H_{\mathrm{ODUT}}^{*}(\omega_{\mathrm{o}}+\Delta\omega)}=H_{\mathrm{ODUT}}(\omega_{\mathrm{o}}+\omega_{\mathrm{e}})+\Delta_1,\ \text{if } \omega_{\mathrm{e}}>\Delta\omega \\ &H_{\mathrm{ODUT}}^{\mathrm{m}}(\omega_{\mathrm{o}}+\omega_{\mathrm{e}})=\frac{i_{\mathrm{m}}(\Delta\omega-\omega_{\mathrm{e}})}{i_{\mathrm{cal}}(\Delta\omega-\omega_{\mathrm{e}})H_{\mathrm{ODUT}}^{*}(\omega_{\mathrm{o}}+\Delta\omega)}=H_{\mathrm{ODUT}}(\omega_{\mathrm{o}}+\omega_{\mathrm{e}})+\Delta_1,\ \text{if } \omega_{\mathrm{e}}<\Delta\omega \\ &H_{\mathrm{ODUT}}^{\mathrm{m}}(\omega_{\mathrm{o}}-\omega_{\mathrm{e}})=\frac{i_{\mathrm{m}}(\omega_{\mathrm{e}}+\Delta\omega)}{i_{\mathrm{cal}}(\omega_{\mathrm{e}}+\Delta\omega)H_{\mathrm{ODUT}}^{*}(\omega_{\mathrm{o}}+\Delta\omega)}=H_{\mathrm{ODUT}}(\omega_{\mathrm{o}}-\omega_{\mathrm{e}})+\Delta_2 \end{aligned} \quad (5)$$

where $H_{\mathrm{ODUT}}^{*}(\omega_{\mathrm{o}}+\Delta\omega)$ is the frequency response of the ODUT at the frequency-shifted carrier, which is a measurable complex constant. Δ_1 and Δ_2 are the measurement errors introduced by the unwanted frequency-shifted carrier, which are given by

Optics EXPRESS

$$\Delta_1=\frac{a_{-1}^{*}b_{-1}H^{*}(\omega_o-\omega_e)H(\omega_o-\Delta\omega)}{a_{+1}b_{+1}^{*}H_{sys}(\omega_o+\omega_e)H_{sys}^{*}(\omega_o+\Delta\omega)H_{ODUT}^{*}(\omega_o+\Delta\omega)}$$
$$\Delta_2=\frac{a_{+1}^{*}b_{-1}H^{*}(\omega_o+\omega_e)H(\omega_o-\Delta\omega)}{a_{-1}b_{+1}^{*}H_{sys}(\omega_o-\omega_e)H_{sys}^{*}(\omega_o+\Delta\omega)H_{ODUT}^{*}(\omega_o+\Delta\omega)} \quad (6)$$

As can be seen from (5), the measured frequency responses are comprised by the actual frequency responses of the ODUT and the unwanted frequency-shifted carrier induced errors, which are complex since they are related to the transmission functions of the ODUT and the measurement system. It is worth to mention that the measurement errors can be generally ignored when the SSR is large, but the errors would not be negligible, for example, when measuring a notch whose depth approaches or higher than the SSR of the OSSB signal.

3. Experimental results and discussions

A proof-of-concept experiment based on the setup shown in Fig. 1(a) is carried out. An optical carrier is generated by a tunable laser source (Agilent N7714A) and sent to a dual-polarization Mach-Zehnder modulator (Fujitsu FTM7977HQA) followed by a polarizer, which can serve as the DD-DPMZM. The RF signal from a vector network analyzer (VNA, R&S ZVA67) is directly sent to a sub-MZM and the LO signal from the VNA is introduced to the other sub-MZM after a 90° hybrid coupler. The frequency of the LO signal is 7 GHz, and the wavelength-fixed OSSB signal has a SSR of 35.6 dB, so the unwanted frequency-shifted carrier is well suppressed and the measurement error introduced by it is ignorable. A sampled FBG is served as the ODUT. Two 40-GHz PD (u^2t XPD2120R) are inserted to convert the optical signals into the photocurrents. The magnitude and phase of the photocurrent in the measurement path are extracted by the VNA referring the photocurrent in the reference path. The optical spectra are measured by an optical spectrum analyzer (OSA, BOSA 400) with a resolution of 0.1 pm.

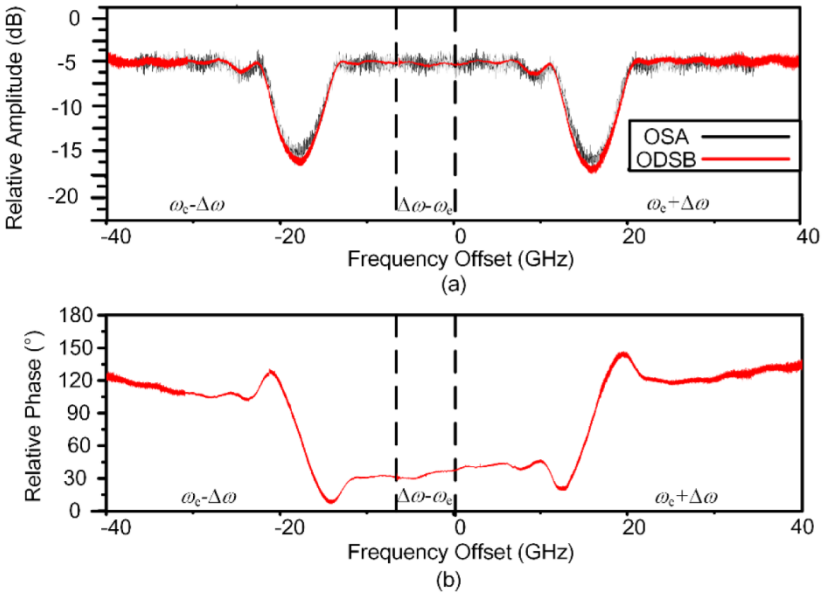

Fig. 2. The (a) magnitude and (b) phase responses of the sampled FBG measured by the proposed ODSB-based OVA.

Figure 2 shows the magnitude and phase responses of the sampled FBG measured by the proposed ODSB-based OVA. Because the frequency of the LO is 7 GHz, the measurement

Optics EXPRESS

range is divided into three segments [f_o–40 GHz, f_o–7 GHz], [f_o–7 GHz, f_o] and [f_o, f_o + 40 GHz], in which the magnitude and phase of the beat notes with frequencies of $\omega_e-\Delta\omega$ ($\omega_e>\Delta\omega$), $\Delta\omega-\omega_e$ ($\omega_e<\Delta\omega$) and $\omega_e+\Delta\omega$ are detected, respectively. Each segment has 60001 points, so the resolutions in the three segments are 486 kHz, 182 kHz, and 667 kHz, respectively. As a comparison, the magnitude response of the sampled FBG measured by an amplified spontaneous emission (ASE) source and the OSA with a resolution of 0.1 pm is also plotted in Fig. 2(a). The magnitude responses measured by the two methods are coincided. It should be noted that the noise in the measured responses grows with the frequency of the RF signal because the signal-to-noise ratios (SNRs) of the two sweeping sidebands decrease with the frequency of the RF signal due to the decrease of the modulation efficiency.

Figure 3 shows the magnitude and phase responses measured by the proposed ODSB-based OVA when the wavelength-fixed OSSB signal has different SSRs. As can be seen, the unwanted frequency-shifted carrier induced measurement errors in the measured magnitude and phase responses become significant when the SSR approaches the notch depth, which agrees well with the analytical analysis. To improve the accuracy of the ODSB-based OVA, the unwanted frequency-shifted carrier of the OSSB signal should be well suppressed.

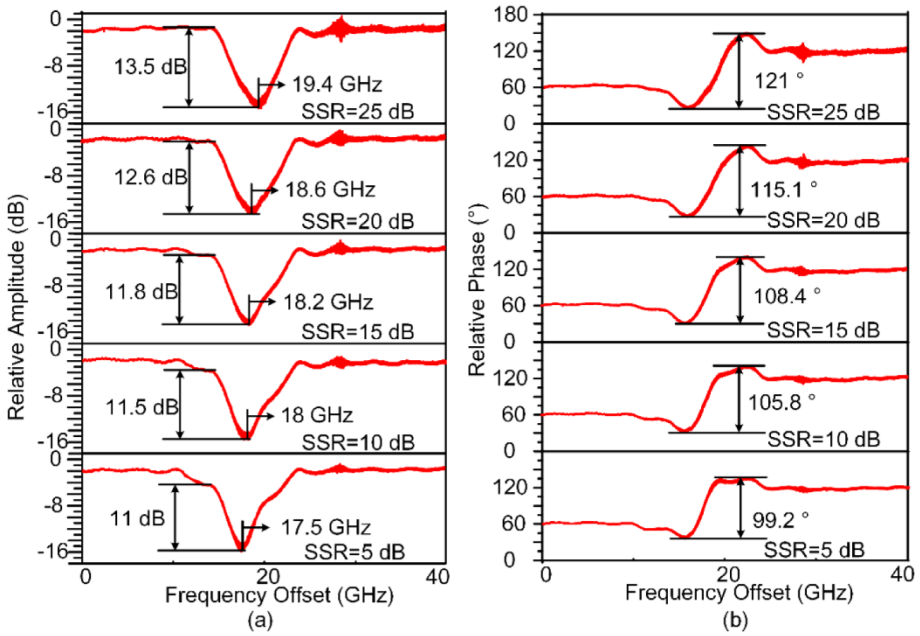

Fig. 3. The (a) magnitude and (b) phase responses measured by the proposed ODSB-based OVA at different SSRs.

4. Conclusion

In conclusion, a high-resolution ODSB-based OVA by use of a DD-DPMZM is proposed and experimentally demonstrated. The magnitude and phase responses of a sampled FBG in a frequency range of 80 GHz are obtained with a resolution less than 667 kHz. The influence of the unwanted frequency-shifted carrier on the measurement accuracy is investigated, showing that the unwanted frequency-shifted carrier should be well suppressed to achieve a high accuracy.

Funding

National Natural Science Foundation of China (61527820, 61422108); Jiangsu Provincial Program for High-level Talents in Six Areas (DZXX-034); “333 Project” of Jiangsu Province

Optics EXPRESS

(BRA2015343); Fundamental Research Funds for the Central Universities; Project Funded by the Priority Academic Program Development of Jiangsu Higher Education Institutions.

157.0.78.110 {ts '2017-02-21 18:58:59'}